Available online at www.sciencedirect.com
SCIENCE DIRECT®
Journal of Photochemistry and Photobiology A: Chemistry 163 (2004) 529–536
Journal of Photochemistry and Photobiology A:Chemistry
www.elsevier.com/locate/jphotochem

Ultrafast photoinduced electron transfer from *N*,*N*,*N*′,*N*′-tetramethyl-*p*-phenylenediamine and *N*,*N*,*N*′,*N*′-tetramethylbenzidine to dichloromethane

Laurent Boilet, Guy Buntinx, Christophe Lefumeux, Olivier Poizat*

Laboratoire de Spectrochimie Infrarouge et Raman (UMR 8516 de l'Université et du CNRS), Centre d'Etudes et de Recherches Lasers et Applications (FR 2416 du CNRS), Bât. C5, Université des Sciences et Technologies de Lille, 59655 Villeneuve d'Ascq, France

Received 5 August 2003; received in revised form 5 December 2003; accepted 18 February 2004

Abstract

The photoinduced reaction of electron transfer (ET) from *N*,*N*,*N*′,*N*′-tetramethyl-*p*-phenylenediamine (TMPD) and *N*,*N*,*N*′,*N*′-tetramethylbenzidine (TMB) to the dichloromethane solvent has been studied by picosecond transient absorption and time-resolved resonance Raman spectroscopy. In neat CH_2Cl_2, "static" quenching of the lowest excited singlet state (S_1) of these amines is demonstrated. For TMPD, the reaction shows two kinetic contributions ($\tau_1 < 4$ ps, $\tau_2 = 9.5$ ps) that are ascribed to the fractions of excited molecules that react before and after they are vibrationally relaxed, respectively. A faster quenching reaction is observed for TMB ($\tau < 4$ ps) although it is less favourable energetically than for TMPD. This result is ascribed to a stronger acceptor–donor electronic coupling in the case of TMB, principally due a larger delocalization of the S_1 state donor orbital. The observation of a partial back electron transfer (9% yield) is tentatively explained as resulting from an evolution of the reaction product from an initial [$TMB^{+\bullet}$, $CH_2Cl_2^{-\bullet}$] ion pair allowing charge recombination to a final form [$TMB^{+\bullet}$, Cl^-] inappropriate to back ET.

Keywords: Aromatic amines; Electron transfer; Time-resolved spectroscopy; Raman

1. Introduction

Due to their low ionisation potential, aromatic amines like *N*,*N*-dimethylaniline (DMA, 7.1 eV), *N*,*N*,*N*′,*N*′-tetramethyl-*p*-phenylenediamine (TMPD, 5.9–6.6 eV), and *N*,*N*,*N*′,*N*′-tetramethylbenzidine (TMB, 6.1–6.8 eV), have been widely used as model compounds to study the ionisation processes in solution. One-photon ionisation has been observed in polar solvents such as methanol, acetonitrile and water [1–6]. However, surprisingly, the most efficient one-photon electron ejection from amines occurs in non-polar halogenated solvents. Transient absorption and time-resolved microwave dielectric absorption experiments in the microsecond time domain revealed that fast formation of the radical cation of TMB [7–9], TMPD [9–13] and DMA [14,15] arises in CCl_4 with high quantum yield.

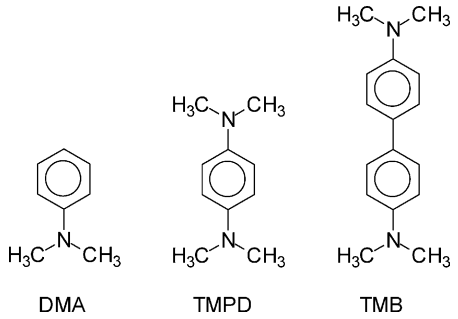

The reaction is suggested to occur in the S_1 state of the amine [7,12,15] but there is no direct experimental evidence to support this hypothesis. It has been assumed that the process leads to the formation of a long-lived contact ion pair (CIP), amine$^{+\bullet}X^-$ (X: halogen atom), most of the energy required for the electron abstraction being brought from the energy gained by forming the ion pair. It has also been suggested that the lowest excited triplet state (T_1) of TMPD can produce a CIP in the presence of a halogenated compound AX in non-polar hydrocarbon solvents via diffusional quenching [13]. In the case of TMB [8,9] and DMA [15], this reaction does not take place but similar ion-pair

* Corresponding author. Tel.: +33-320434085; fax: +33-320336354.
E-mail address: poizat@univ-lille1.fr (O. Poizat).

1010-6030/$ – see front matter © 2004 Elsevier B.V. All rights reserved.
doi:10.1016/j.jphotochem.2004.02.011

formation has been suggested to occur by direct excitation of weakly-bound van der Waals (amine·AX) complexes pre-existing in the ground state.

In this paper, we present the first time-resolved spectroscopic investigation in the picosecond time domain of the photoinduced electron transfer (ET) from TMB and TMPD to a halogenated solvent, dichloromethane. Measurements are done by using the two complementary pump-probe spectroscopic techniques of transient UV-visible absorption and time-resolved resonance Raman scattering. The results are interpreted with the help of previous analyses of the transient absorption and resonance Raman spectra of the TMB and TMPD excited S_1 state [16–18] and radical cation [19–22] species that have been well identified. It is known that the absorption spectra of the radical cation [20] and T_1 state [23] of TMPD on one hand, and of the radical cation [19], S_1 state [16] and T_1 state [19] of TMB on the other hand, are quite similar in such a way that they do not allow distinguishing clearly these species from each others. Raman spectra being much more specific, they lead to much better characterisation and discrimination of the different species, allowing a more accurate investigation of the reaction path. The implication of the lowest excited singlet state (S_1) in the fast photoinduced formation of the TMB and TMPD radical cation in CH_2Cl_2 will be demonstrated.

2. Experimental

TMB and TMPD were purchased from Aldrich. All samples were sublimed in vacuo prior to each spectroscopic measurement. CH_2Cl_2 and *n*-hexane (SDS, spectroscopic grade) were used as received. All measurements were performed on 1×10^{-3} M solutions. The subpicosecond transient absorption and picosecond Raman scattering experiments have already been described [24–26]. Briefly, they were carried out by using a 1 kHz Ti-sapphire laser system based upon a Coherent (MIRA 900 D) oscillator and a BM Industries (ALPHA 1000) regenerative amplifier. This system was set in a femtosecond configuration for all the absorption measurements. Tripling the initial 90 fs pulses at 800 nm (0.5 mm BBO crystal) provided the pump excitation at 266 nm. A probe white light continuum pulse was generated at 800 nm in a CaF_2 plate. The probe pulse was delayed in time relative to the pump pulse using an optical delay line (Microcontrol model MT160-250PP driven by an ITL09 controller, precision ±1 μm). The overall time resolution (fwhm of the pump-probe cross-correlation) is estimated to be about 300 fs from the two photon (pump + probe) absorption signal in pure *n*-hexane. The time dispersion of the continuum light over the spectral range analysed (400–750 nm) is about 0.8 ps. The transmitted light was analysed by a CCD camera (Princeton Instrument LN/CCD-1340/400-EB detector + ST-138 controller). Samples were circulating in a flow cell with 2.5 mm optical path length. Data were accumulated over 3 min (∼180,000 pump-probe sequences).

For the Raman measurements, the laser source was set in a picosecond configuration. The output wavelength was set at 752 nm for the probe excitation. Pump pulses at 250.6 nm were obtained by tripling the 752 nm fundamental. The pump-probe cross-correlation fwhm was ∼4 ps. Scattered light was collected at 90° to the incident excitation and sent through a Notch filter into a home-built polychromator coupled to a CCD camera (Princeton Instrument LN/CCD-1100-PB-UV/AR detector + ST-138 controller). The flowing jet sampling technique was adopted (1 mm diameter jet). The wavenumber shift was calibrated using the Raman spectrum of indene. Data collection times were ∼10 min. In all absorption and Raman measurements, the pump-probe polarisation configuration was set at the magic angle. We must mention an artifact of measurement observed in the spectra when utilising a too intense probe excitation. This artifact arises in case of probing in strong resonance conditions (probe wavelength tuned in a region of strong absorption of the probed species) but does not concern the out-of-resonance and low resonance Raman spectra (probe excitation set in a region of low absorption of the probed species). It is manifested by a notable broadening of the Raman bands and a non-linear response of the Raman intensities to changes in the probe power. Kinetic measurements become then erroneous. This artifact has already been reported by several researchers and ascribed to a local heating of the probed molecules due to a saturation effect [27]. Therefore, all measurements were made with low probe-laser intensity (∼0.3 μJ, spot diameter ∼100 μm).

3. Results and discussion

The existence of van der Waals ground state complexes between the amines TMPD and TMB and halogenated alkanes has been suggested [8,9]. A charge-transfer complex between aniline and CCl_4 has been evidenced by absorption in cyclohexane [28] and benzene [15] solutions. In order to check an eventual charge-transfer interaction between CH_2Cl_2 and TMPD or TMB, we have measured the UV absorption spectrum of these amines in *n*-hexane, CH_2Cl_2, and various *n*-hexane/CH_2Cl_2 mixtures. These data do not show any significant spectral change with the addition of CH_2Cl_2 in *n*-hexane. There is thus no spectroscopic evidence for the formation of (amine–CH_2Cl_2) charge-transfer complexes in the ground state.

3.1. *N,N,N′,N′-tetramethyl-p-phenylenediamine*

Femtosecond transient absorption spectra recorded in the 0.6–10 ps time delay range following 266 nm excitation of TMPD in CH_2Cl_2 (1×10^{-3} M) are presented in Fig. 1. The 10 ps spectrum shows one band with two maxima at 567 and 614 nm and a shoulder around 525 nm. It is typical of the radical cation $TMPD^{+\bullet}$ [20]. No spectral evolution is observed from 10 to 1500 ps. Between 0.6 and 10 ps, a

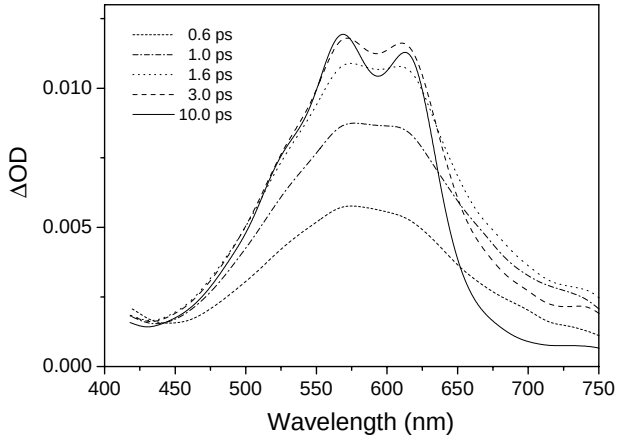

Fig. 1. Transient absorption spectra of TMPD (1×10^{-3} M) in CH_2Cl_2 at different time delays (0.6–10 ps) after 266 nm excitation.

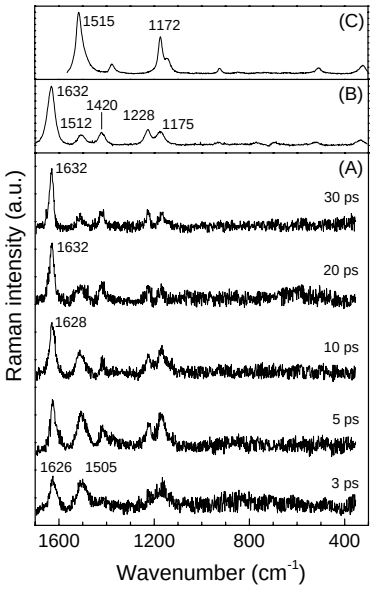

Fig. 2. Time-resolved resonance Raman spectra (A) of a solution of TMPD (1×10^{-3} M) in CH_2Cl_2 at different times after excitation at 250.6 nm ($\lambda_{probe} = 752$ nm), (B) of the TMPD radical cation in acetonitrile ($\lambda_{pump} = 266$ nm, $\lambda_{probe} = 647$ nm, delay = 1 ns) [22], and (C) of the TMPD S_1 state in methanol ($\lambda_{pump} = 250.6$ nm, $\lambda_{probe} = 752$ nm, delay = 30 ps) [18].

progressive narrowing and an increase in the structure of the absorption band is observed whereas the intensity at the band maximum increases. We assume that this transient absorption signal is mainly due to the radical cation. Its evolution in the 0.6–10 ps time range can be assigned to vibrational relaxation and/or solvation processes. It is possible that the short-time red tail involves a contribution of the first excited singlet state absorption spectrum. Indeed, the vibrationally relaxed S_1 state is characterised in *n*-hexane by a broad band with vibronic maxima at 610, 660 and 725 nm [20,29]. As observed for the radical cation, the unrelaxed S_1 state spectrum is much less structured [29]. However, there is no clear evidence to support or reject the presence of a S_1 state contribution to the spectral evolution in Fig. 1. Moreover, in the hypothesis that S_1 is present, its decay would occur in this 0–10 ps time domain, which also corresponds to the period of vibrational relaxation of both the radical cation and S_1 state species. The spectral evolution in this time domain is thus expected to result from the complex superposition of relaxation effects and population changes, in such a way that no reliable kinetic information can be inferred concerning the formation of the radical cation.

Fig. 2 (part A) shows the time evolution of the time-resolved resonance Raman spectra probed at 752 nm, that is, in good resonance conditions for the S_1 state but almost out of resonance for the radical cation [20]. In order to limit as much as possible the two-photon processes, usually favoured in Raman experiments since the excitation is more tightly focused in the sample, the pump intensity was maintained at a level (1.8 μJ, spot diameter ∼100 μm) for which no Raman band from the $TMPD^{+\bullet}$ species was detected in a solution of TMPD in *n*-hexane. Since in this inert solvent TMPD does not undergo one-photon ionisation [29], the absence of any radical band means that the excitation conditions are unfavourable to two-photon ionisation. For comparison, reference Raman spectra probed in optimum resonance conditions for the radical cation (pump 266 nm, probe 647 nm) [22] and the S_1 state (pump 250.6 nm, probe 752 nm) [18] are also given in Fig. 2, parts B and C, respectively. The 30 ps spectrum in part A is unambiguously characteristic of the TMPD radical cation. In the 3 ps spectrum, the radical cation species is already present and identified by the 1626 cm^{-1} Raman line. However the two bands at 1505 and 1170 cm^{-1} are too intense to correspond to the radical cation lines lying in these regions (1512 and 1175 cm^{-1}, respectively) and are rather ascribed to the TMPD first excited singlet state. It is worth remarking that, although the 1626 and 1505 cm^{-1} bands have approximately the same intensity at 3 ps, the fact that the resonance Raman conditions at 752 nm are much more favourable to the S_1 state implies that the amount of $TMPD^{+\bullet}$ present at 3 ps is considerably higher than the amount of S_1 state. It is thus not surprising that the singlet state species has not been clearly distinguished by transient absorption spectroscopy. The resonance Raman spectra appear to be much more useful than the absorption spectra for characterising weakly concentrated species in complex mixtures. The quantum yield of formation of the S_1 state upon 266 nm excitation in CH_2Cl_2 appears much weaker than in *n*-hexane, methanol or acetonitrile [29]. As the delay time is increased, the decay of the S_1 state signal is manifested by the decrease in intensity of the 1505 and 1170 cm^{-1} bands. The time evolution of the radical cation and S_1 state species has been monitored by plotting the Raman intensity of the 1626 and 1505 cm^{-1} bands, respectively, as a function of time (Fig. 3). Since the 1505 cm^{-1} band contains a weak contribution from the radical cation line at 1512 cm^{-1} (see Fig. 2, part B), this contribution was estimated at each time

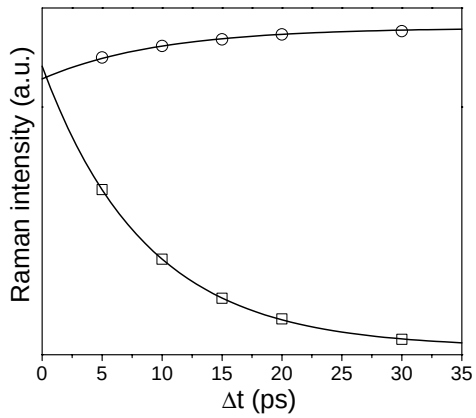

Fig. 3. Plots of the time-dependent Raman intensity of the $TMPD^{+\bullet}$ band at 1626 cm^{-1} (○) and of the S_1 state contribution (see the text) to the 1505 cm^{-1} band (□) measured following 250.6 nm excitation of a solution of TMPD (1×10^{-3} M) in CH_2Cl_2. The full lines are the best fits to mono-exponential kinetics ($\tau = 9.5$ ps).

relative to the 1626 cm^{-1} band intensity, then subtracted from the intensity of the 1505 cm^{-1} line to determine the real S_1 state contribution plotted in Fig. 3. The radical cation evolution shows clearly two distinct components: an instantaneous rise (∼85%) followed by a slower increase (∼15%) up to 30 ps. The TMPD S_1 state disappears within 30 ps. The slow radical cation growth and S_1 state decay can both be fitted by the same mono-exponential kinetics with a characteristic time of 9.5 ps (solid curves in Fig. 3). The short S_1 state lifetime of TMPD in CH_2Cl_2 compared to that reported in other organic solvents (1.2 ns in acetonitrile [30], 4.3 ns in methanol [31], 4.2 ns in *n*-hexane [17]) is thus due to very efficient quenching by electron transfer to the solvent. Note that the frequency of the radical cation mode of highest energy increases with time from 1626 to 1632 cm^{-1} at 3 and 20 ps. This shift parallels the sharpening of the $TMPD^{+\bullet}$ absorption band (Fig. 1). It is thus ascribed by analogy to vibrational relaxation.

In summary, the photophysics of TMPD in CH_2Cl_2 following pulse excitation at 266 nm is characterised by two essential observations: (i) the apparent S_1 state yield is extremely weak compared to that observed in non-chlorinated solvents. This result can be related to the high yield (85%) of $TMPD^{+\bullet}$ cation that is produced instantaneously. It indicates that most of the S_1 state species are likely quenched by CH_2Cl_2 to produce the radical cation with a characteristic time much shorter than the 4 ps time resolution of our experiment. (ii) The small fraction of the S_1 state population that has not been consumed in this fast process is quenched in 9.5 ps by electron transfer to the solvent to yield 15% of the produced $TMPD^{+\bullet}$ cation. This time is somewhat larger than the 4.5 ps diffusion time determined for CH_2Cl_2 from the diffusion-controlled rate constant ($\tau_{diff} = 1/k_{diff}$) calculated from the Smoluchowski equation [32]. However, since photolysis occurs in the neat solvent, the S_1 state molecules are surrounded by a number of potential electron acceptors and no diffusion is necessary. In that sense, the reaction is the analogue of the more frequently studied intermolecular ET reaction where the solvent acts as electron donor [33–40]. The 9.5 ps time constant found above is significantly longer than the fastest (barrierless) processes reported for electron donation from a solvent (∼100 fs [36,38,39]), indicating that some barrier exists to the abstraction of electron from S_1 TMPD by CH_2Cl_2.

The observation of two quenching time constants, $\tau_1 < 4$ ps and $\tau_2 = 9.5$ ps, can be compared to the results reported for the photoinduced ET in electron-donating solvents. In fact, in case of low activation barrier processes, the reaction evolution is generally highly non-exponential and reasonably well fitted by bi-exponential kinetics with the faster rate being 5–10 times higher than the slower one [33–37,40,41]. Non-exponentiality in the ET process is frequently assumed to result from a distribution of reaction rates related to an initial distribution of mutual configurations (distances and relative orientations) of the donor and acceptor reactants [34–37,40,41]. This arises because different configurations are characterised by different magnitudes of the electronic coupling (intermolecular orbital overlap) [37,40] or of the activation barrier (due to different values of the free energy gap ΔG° between reactants and products) [36]. However such non-exponential behaviour can occur only for ET processes faster than the solvent relaxation time τ_S^{-1}. If the solvation dynamics is faster than ET, the initial distribution is randomised and thus cannot induce non-exponentially. In this regard, it is convenient to define, as other authors, a weighted average reaction time constant as $\langle \tau \rangle = a_1\, \tau_1 + a_2 \tau_2$. Assuming a lower limit of $\tau_1 \sim \tau_2 \times 0.1 = 0.95$ ps and setting the a_1 and a_2 parameters to 0.85 and 0.15, respectively, according to the relative amplitudes found for the instantaneous and slow rising components of $TMPD^{+\bullet}$, leads to a minimum value of the average ET rate of ∼2 ps. This value is notably higher than the solvent relaxation time values of 0.4 ps [42] or 0.56 ps [43] reported for CH_2Cl_2. Ascribing the apparent bi-exponential character of the kinetics of electron transfer from S_1 TMPD to CH_2Cl_2 to inhomogeneities in the solvent solute mutual configuration appears thus questionable.

A more plausible interpretation of the observed kinetics is that there is a distribution of reaction rates related to a time-dependent distribution of vibrational levels in the excited S_1 state of TMPD. In fact, the 250.6 nm excitation used in our time-resolved Raman experiments lies at a notably higher energy than the maximum of the ground state absorption band of lowest energy (315 nm [44]). The S_1 state molecules are thus initially created with a significant excess of vibrational energy and vibrational relaxation must take place in a picosecond time scale. In *n*-hexane, where S_1 TMPD is long-lived ($\tau_{S1} = 4.2$ ns), vibrational relaxation results in a manifest sharpening of the vibronic band structure in the visible $S_1 \rightarrow S_n$ absorption and a characteristic time of $\tau_{vr} \sim 8$ ps has been measured [29]. Since the vibrationally

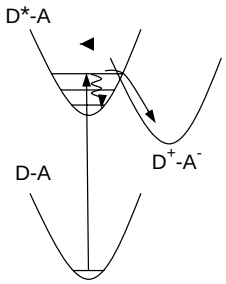

Scheme 1.

excited molecules have lower activation barrier for ET than the vibrationally relaxed molecules (see Scheme 1), the ET reaction rate is expected to decrease as the vibrational relaxation proceeds. It is possible that the excess vibrational energy deposited in the molecule brings the system in a region of the energy surface where the barrier is strongly attenuated relative to its magnitude in the relaxed configuration. In this regard, the 9.5 ps time can be ascribed to the reaction occurring in the bottom of the S_1 state potential (τ^0_{ET}) whereas the unresolved fast kinetics might characterise an average value for the ET reaction involving hot molecules (τ^v_{ET}). Fast quenching of hot molecules is competing with vibrational relaxation (τ_{vr}). Accordingly, the 0.85:0.15 ratio of the fast (unresolved) and slow rising components of $TMPD^{+\bullet}$ must correspond approximately to the quantum yield ratio $\Phi^v_{ET}/\Phi^0_{ET} = \tau^v_{ET}/\tau_{vr}$. Assuming $\tau_{vr} = 8$ ps as in hexane, an average ET time constant of $\tau^v_{ET} = 1.4$ ps and a mean lifetime of $\tau^v = 1/((\tau_{vr})^{-1} + (\tau^v_{ET})^{-1}) = 1.2$ ps are deduced for the vibrationally excited S_1-state population. It should be possible to confirm the above interpretation by doing measurements with a pump excitation tuned in the 330–350 nm domain corresponding to the position of the $S_0 \rightarrow S_1$ $E_{0–0}$ transition of TMPD in order to suppress the excess of vibrational energy. Unfortunately, adjusting the pump excitation wavelength is not possible with our present experimental set-up. A non-collinear optical parametric amplification device is planed to be developed in the near-future to allow such experiments.

3.2. *N,N,N′,N′*-tetramethylbenzidine

Transient absorption spectra recorded for different time delays between 0.8 and 700 ps after 266 nm photoexcitation of a solution of TMB (1×10^{-3} M) in CH_2Cl_2 are presented in Fig. 4. The 700–1000 nm spectral region has also been probed but is not shown here since the signal-to-noise ratio in this region was worse and no supplementary information could be obtained. The spectra in Fig. 4 show at all times a band centred around 455 nm. Almost structureless below 3 ps, this band narrows progressively up to 20 ps whereas three vibronic maxima at 435, 455 and 470 nm appear. No further spectral evolution is observed after 20 ps. The 20 ps spectrum corresponds unambiguously to the TMB

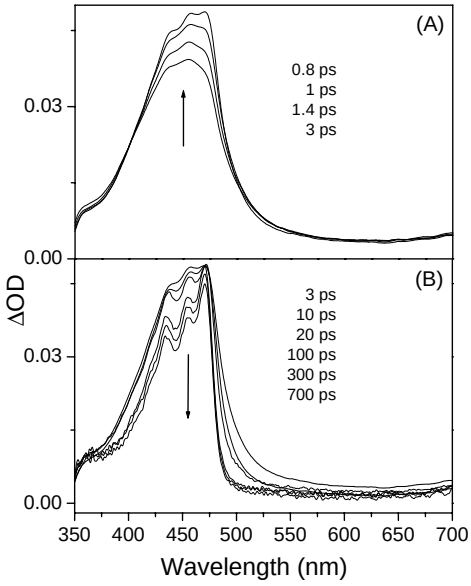

Fig. 4. Transient absorption spectra of TMB (1×10^{-3} M) in CH_2Cl_2 at different time delays (A: 0.8–3 ps; B: 3–700 ps) after 266 nm excitation.

radical cation spectrum [19]. The band intensity increases between 0.8 and 3 ps, then decreases by about 9% with a characteristic time of 70 ps before stabilising. The S_1 state of TMB is characterised by a structureless band peaking around 440 nm [16,29], almost coincident with the radical cation band. Therefore, as in the case of TMPD, it is not clear whether the short-time spectral changes observed in Fig. 4 are exclusively due to the relaxation of $TMB^{+\bullet}$ or involve a contribution of the S_1 state dynamics. The same uncertainty was found in the 700–1000 nm region where both the S_1 state and radical cation species have superimposed absorption bands.

Time-resolved resonance Raman measurements were performed on solutions of TMB (1×10^{-3} M) in neat CH_2Cl_2, in various *n*-hexane/CH_2Cl_2 mixtures, and in neat *n*-hexane, for different pump-probe time delays in the 0–1500 ps range. The probe wavelength at 752 nm was in resonance with the red absorption band of both the S_1 state and radical cation of TMB. An intense fluorescence emission in the 400–500 nm region prohibited any Raman measurement using a probe excitation in resonance with the strong absorption band observed for these species around 450 nm. As in the case of TMPD, the pump excitation energy (1.8 μJ) was sufficiently low to avoid any significant two-photon ionisation of TMB in *n*-hexane. In the following, we focus the discussion on the 1400–1700 cm^{-1} frequency domain of the transient Raman spectra, which is an essential fingerprint region for both the S_1 state [18] and radical cation species [21]. Fig. 5 (part A) shows the time-resolved Raman spectrum obtained in CH_2Cl_2 at a time delay of 0 ps (coincident pump and probe pulses). This spectrum is typical of the radical cation $TMB^{+\bullet}$ [21] and does not present any Raman band ascribable to the S_1 state. The same spectrum is observed at all times in the 0–1500 ps range, with an approximately constant

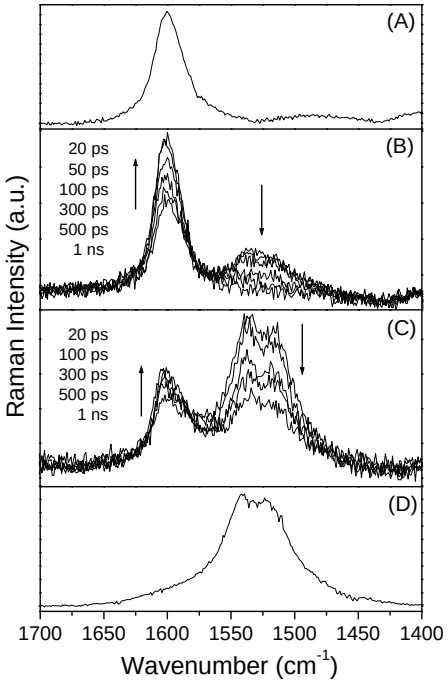

Fig. 5. Time-resolved resonance Raman spectra of (A) a solution of TMB (1×10^{-3} M) in CH_2Cl_2 at zero picosecond pump-probe time delay. (B) and (C) Solutions of TMB (1×10^{-3} M) in 75/25 and 90/10 *n*-hexane/CH_2Cl_2 mixtures, respectively, at different pump-probe time delays. (D) The TMB S_1 state obtained 10 ps after excitation of a solution of TMB in *n*-hexane [18]; $\lambda_{pump} = 250.6$ nm and $\lambda_{probe} = 752$ nm in all cases.

intensity. Parts B and C in Fig. 5 show spectra recorded from 20 to 1000 ps in *n*-hexane solutions containing 25 and 10% CH_2Cl_2 (v/v), respectively. These spectra present, in addition to the 1602 cm^{-1} line already seen in pure CH_2Cl_2 (part A), characteristic of the radical cation, a double band lying around 1525 cm^{-1}, representative of the S_1 state of TMB [18]. For comparison, the spectrum recorded in neat *n*-hexane at a time delay of 10 ps is shown in part D of Fig. 5. This spectrum corresponds exclusively to the S_1 state. Its intensity does not change much on the 0–1000 ps time domain, in agreement with the ~10 ns lifetime reported for S_1 TMB in *n*-hexane [45].

The time dependence of the radical cation band intensity shows two distinct components: an instantaneous, unresolved rise (initial band intensity) and a slow growth. The latter is observed only in the binary solvent mixtures and parallels the decay of the S_1 state band. Both events can be fitted by the same single exponential function, with a time constant decreasing from 500 ± 50 to 150 ± 50 ps on going from 10 to 25% CH_2Cl_2 in *n*-hexane. This result and the notable shortening of the S_1 lifetime compared to its value in neat *n*-hexane (10 ns) demonstrates definitely the existence of a diffusional excited state quenching of TMB by electron transfer to CH_2Cl_2 (average k_q^{dif} value of 2.3×10^{10} s^{-1}). However, the relative magnitude of the increase in intensity of the radical cation band from 20 to 1000 ps compared to the amplitude of the S_1 band decay on the same time period is notably lowered on going from the 25 to the 10% CH_2Cl_2 solution. This observation indicates that the apparent quantum yield of formation of the radical cation does not follow the quantum yield of quenching of the S_1 state but decreases significantly in the *n*-hexane rich solvent composition domain. It suggests that, in this domain, part of the ions produced in the S_1 state quenching reaction undergo immediate charge recombination. As stated above (section introduction), photoinduced ET from aromatic amines to chlorinated hydrocarbons is assumed to yield an ion pair [7–15]. It is conceivable that the stabilisation by solvation of the ion pair requires a minimum number of CH_2Cl_2 molecules. On going to the *n*-hexane rich region of the solvent mixture composition, there is an increasing probability for the ion pair to be produced in an environment where the above threshold is not reached. In this case, it can be envisaged that deactivation of S_1 TMB by CH_2Cl_2 still occurs but is immediately followed by charge recombination, in such a way that the reaction is unproductive.

Consider now the contribution of $TMB^{+\bullet}$ that is produced instantaneously upon excitation (initial band intensity). This contribution is observed in the CH_2Cl_2/*n*-hexane mixtures as well as in neat CH_2Cl_2, in which case it represents 100% of the produced cation. It can be seen in Fig. 5 (parts B and C), that the ratio of the radical cation to S_1 state initial band intensity (20 ps spectra) increases importantly on going from the 10 to 25% CH_2Cl_2 solution. In pure CH_2Cl_2, the S_1 state is not observed at all. This inverse correlation between the initial $TMB^{+\bullet}$ and S_1 state yields indicates that the fast, unresolved process of formation of the TMB radical cation results from non-diffusional, "static" quenching of the S_1 state by surrounding CH_2Cl_2 molecules in direct contact. This process is likely favoured by the high acceptor concentration in the measured solutions. It is analogous to the ET transfer reaction observed above for TMPD in neat CH_2Cl_2. The data show an increase of the initial $TMB^{+\bullet}$ yield with increasing CH_2Cl_2 concentration, which is consistent with the fact that the larger the acceptor concentration, the higher the probability of finding acceptor–donor pairs in suitable configuration for ET. Whereas the "static" S_1-state quenching in pure CH_2Cl_2 has been characterised by two kinetic contributions with time constants of $\tau_1 < 4$ and $\tau_2 = 9.5$ ps in the case of TMPD, it is entirely faster than the 4 ps time resolution of our Raman experiment in the case of TMB. This means that the ET reaction between S_1 TMB and CH_2Cl_2 is completed before vibrational relaxation takes place. A faster quenching reaction for TMB than for TMPD cannot be explained on the basis of driving force arguments. In fact, both amines have similar S_0–S_1 energy gaps ($\lambda_{max}(S_0$–$S_1) = 300$ and 315 nm for TMB and TMPD, respectively) but the oxidation potential of TMB (+0.32 V versus SCE in CH_3CN [46]) is twice that of TMPD (+0.16 V versus SCE in CH_3CN [46]). A lower free energy gap ΔG° between reactants and products, i.e. a higher activation barrier for ET, is thus expected for TMB. Therefore, one might assume that, in the case of TMB, there is a greater electronic coupling between

the reactants. In fact, Castner et al. [37] and Morandeira et al. [40] have recently shown that, in case of reacting solvent, the numerous solvent molecules in contact with the excited solute have very different probabilities for ET, the mutual orientation of the two species playing a crucial role in determining the magnitude of their orbital overlap. From a vibrational analysis of the S_1 state of TMPD and TMB based on time-resolved resonance Raman data [18], it has been established that both excited species have planar structures with the amino groups in a sp^2 configuration due to the interaction of the nitrogen lone pair of electrons with the π electron system of the rings. This nπ conjugation, already present in the ground state [47], is slightly reinforced in the S_1 state. It is responsible for a partial π-character of the N-ring bonds and a large delocalization of the π-type orbitals. In this regard, the major difference between the TMPD and TMB S_1 state electronic distributions is the fact that the area covered by this delocalized π-network in TMB is almost twice that in TMPD. We suggest thus that the faster quenching dynamics of TMB is mainly due to a larger number of electron-accepting solvent molecules that can have the right orientation and distance for ET rather than to a radical increase in magnitude of the electronic coupling itself. Note that the static quenching rate in pure CH_2Cl_2 ($k_q^{st} > 2.5 \times 10^{11}\,s^{-1}$) is an order of magnitude faster than the bimolecular rate of $k_q^{dif} \times [CH_2Cl_2] = 2.3 \times 10^{10}\,s^{-1}$ expected from the diffusional quenching rate constant k_q^{dif} found above in the CH_2Cl_2/*n*-hexane solvent mixtures. This observation confirms the existence, in pure CH_2Cl_2, of specific mutual orientations and distances of the electron donor and acceptor that allow high electronic coupling, in agreement with the reports of Castner et al. [37] and Morandeira et al. [40].

A last point to discuss concerns the ~9% decay (τ~70 ps) of the radical cation absorption band observed in neat CH_2Cl_2 before its stabilisation (this minor effect was not apparent in the time evolution of the Raman spectra). This decay indicates that partial charge recombination takes place at short-time. Assuming that the final reaction product is a long-lived ion pair [$TMB^{+\bullet}$, Cl^-] [7–15] in which back electron transfer cannot occur, the observed 70 ps dynamics can be associated to the evolution from an initial ion pair structure allowing charge recombination to this long-lived ion pair. This evolution can be tentatively ascribed to the dissociation of the CH_2Cl_2 anion radical, i.e., to the passage from an initial [$TMB^{+\bullet}$, $CH_2Cl_2^{-\bullet}$] ion pair to the [$TMB^{+\bullet}$, Cl^-] pair. In this assumption, the dynamics of $CH_2Cl_2^{-\bullet}$ dissociation ($k_{dis} \sim 1.3 \times 10^{10}\,s^{-1}$, $\tau_{dis} \sim 77$ ps) is competing with the charge recombination ($k_{rec} \sim 1.0 \times 10^9\,s^{-1}$).

4. Conclusions

Photoinduced electron transfer from the TMPD and TMB aromatic diamines to the CH_2Cl_2 solvent has been studied by transient absorption and time-resolved resonance Raman spectroscopy in the picosecond time domain. The resonance Raman data demonstrate that the reaction in neat CH_2Cl_2 is due to "static" quenching of the lowest excited singlet state of the amine. For TMPD, the quenching kinetics is characterised by an ultrafast, unresolved component ($\tau_1 < 4$ ps, 85%) and a weaker one ($\tau_2 = 9.5$ ps, 15%). These two contributions are ascribed to the fractions of excited molecules that react before and after they are vibrationally relaxed, respectively, assuming notably different activation barrier for ET in both cases. For TMB, the kinetics of static quenching is entirely faster than the experimental time resolution although the reaction is less favourable energetically than for TMPD. A greater donor–acceptor overall electronic coupling, principally due a more extended delocalization of the S_1 state donor orbital in TMB compared to TMPD, allowing a larger number of quenching solvent molecules to interact, is presumed to account for the observed faster quenching. In the case of TMB, partial charge recombination (time constant 70 ps, yield 9%) is observed to take place within the ion pair before its stabilisation. This result is tentatively explained by an evolution of the reaction product from an initial [$TMB^{+\bullet}$, $CH_2Cl_2^{-\bullet}$] ion pair, allowing intrapair back ET, to the final, long-lived ion pair [$TMB^{+\bullet}$, Cl^-] inappropriate to back ET. In this hypothesis, a dissociation rate of $(77\,ps)^{-1}$ is inferred for $CH_2Cl_2^{-\bullet}$.

Acknowledgements

The authors thank the Groupement de Recherche GDR 1017 from CNRS and the Centre d'Etudes et de Recherche Lasers et Applications (CERLA) for their help in the development of this work. CERLA is supported by the Ministère chargé de la Recherche, Région Nord/Pas de Calais, and the Fonds Européen de Développement Economique des Régions (FEDER).

References

[1] S. Nakamura, N. Kanamaru, S. Nohara, H. Nakamura, Y. Saito, J. Tanaka, M. Sumitani, N. Nakashima, K. Yoshihara, Bull. Chem. Soc. Jpn. 57 (1984) 145.
[2] T. Saito, K. Haida, Y. Hirata, N. Mataga, J. Phys. Chem. 90 (1986) 4017.
[3] M. Lee, D. Jang, D. Kim, S.S. Lee, B.H. Boo, Bull. Korean Chem. Soc. 12 (1991) 429.
[4] Y. Hirata, Y. Tanaka, N. Mataga, Chem. Phys. Lett. 193 (1992) 36.
[5] Y. Hirata, N. Mataga, Prog. React. Kinet. 18 (1993) 273.
[6] F. Saito, S. Tobita, H. Shizuka, J. Photochem. Photobiol. A 106 (1997) 119.
[7] H. Shimamori, Y. Tatsumi, J. Phys. Chem. 97 (1993) 9408.
[8] H. Shimamori, T. Okuda, J. Phys. Chem. 98 (1994) 2576.
[9] H. Shimamori, H. Musasa, J. Phys. Chem. 99 (1995) 14359.
[10] W.C. Meyer, J. Phys. Chem. 74 (1970) 2118.
[11] J.M. Warman, R.J. Visser, Chem. Phys. Lett. 98 (1983) 49.
[12] H. Shimamori, H. Uegaito, J. Phys. Chem. 95 (1991) 6218.
[13] H. Shimamori, K. Hanamuro, Y. Tatsumi, J. Phys. Chem. 97 (1993) 3545.

[14] H. Shimamori, A. Sato, J. Phys. Chem. 98 (1994) 13481.
[15] H. Shimamori, H. Musasa, J. Phys. Chem. 100 (1996) 5343.
[16] Y. Hirata, Y. Mori, N. Mataga, Chem. Phys. Lett. 169 (1990) 427.
[17] Y. Hirata, A. Nogata, N. Mataga, Chem. Phys. Lett. 189 (1992) 159.
[18] L. Boilet, G. Buntinx, C. Lefumeux, O. Poizat, J. Phys. Chem. A 107 (2003) 8506.
[19] Y. Hirata, M. Takimoto, N. Mataga, Chem. Phys. Lett. 97 (1983) 569.
[20] Y. Hirata, M. Ichikawa, N. Mataga, J. Phys. Chem. 94 (1990) 3872.
[21] L. Boilet, G. Buntinx, C. Lapouge, C. Lefumeux, O. Poizat, Phys. Chem. Chem. Phys. 5 (2003) 834.
[22] O. Poizat, A. Bourkba, G. Buntinx, A. Deffontaine, M. Bridoux, J. Chem. Phys. 87 (1987) 11.
[23] Y. Hirata, N. Mataga, J. Phys. Chem. 89 (1985) 4031.
[24] G. Buntinx, R. Naskrecki, O. Poizat, J. Phys. Chem. 100 (1996) 19380.
[25] C. Didierjean, V. Dewaele, G. Buntinx, O. Poizat, Chem. Phys. 237 (1998) 169.
[26] C. Didierjean, G. Buntinx, O. Poizat, J. Phys. Chem. A 102 (1998) 7938.
[27] (a) K. Iwata, H. Hamaguchi, J. Raman Spectrosc. 25 (1994) 615;
(b) T. Nakabayashi, H. Okamoto, M. Tasumi, J. Phys. Chem. A 102 (1998) 9686;
(c) T. Nakabayashi, S. Kamo, H. Sakuragi, N. Nishi, J. Phys. Chem. A 105 (2001) 8605;
(d) K. Iwata, Bull. Chem. Soc. Jpn. 75 (2002) 1075.
[28] W. Boszczyk, T. Latowski, Z. Naturforsch. 44b (1989) 1585.
[29] L. Boilet, PhD Thesis, Lille, 2002.
[30] Y. Hirata, N. Mataga, J. Phys. Chem. 87 (1983) 1680.
[31] Y. Hirata, N. Mataga, J. Phys. Chem. 87 (1983) 3190.
[32] N.J. Turro, Modern Molecular Photochemistry, The Benjamin/Cummings Publishing Company, Menlo Park, 1978.
[33] N. Nagasawa, A.P. Yartsev, K. Tominaga, A.E. Johnson, K. Yoshihara, J. Am. Chem. Soc. 115 (1993) 7922.
[34] K. Yoshihara, K. Tominaga, N. Nagasawa, Bull. Chem. Soc. Jpn. 68 (1995) 696.
[35] H. Shirota, H. Pal, K. Tominaga, K. Yoshihara, Chem. Phys. 236 (1998) 355.
[36] I.V. Rubtsov, H. Shirota, K. Yoshihara, J. Phys. Chem. A 103 (1999) 1801.
[37] E.W. Castner, R. Kennedy, R.J. Cave, J. Phys. Chem. A 104 (2000) 2869.
[38] M. Seel, S. Entleitner, W. Zinth, Chem. Phys. Lett. 275 (1997) 363.
[39] Q.H. Xu, G.D. Scholes, M. Yang, G.R. Fleming, J. Phys. Chem. A 103 (1999) 10348.
[40] A. Morandeira, A. Fürstenberg, J.C. Gumy, E. Vauthey, J. Phys. Chem. A 107 (2003) 5375.
[41] D.R. James, W.R. Ware, Chem. Phys. Lett. 120 (1985) 455.
[42] T. Gennett, D.F. Miller, M.J. Weaver, J. Phys. Chem. 89 (1985) 2787.
[43] M.L. Horng, J.A. Gardecki, A. Papazyan, M. Maroncelli, J. Phys. Chem. 99 (1995) 17311.
[44] A.C. Albrecht, W.T. Simpson, J. Am. Chem. Soc. 77 (1955) 4454.
[45] S. Hashimoto, J.K. Thomas, J. Phys. Chem. 88 (1984) 4044.
[46] G.J. Kavarnos, N.J. Turro, Chem. Rev. 86 (1986) 401.
[47] V. Guichard, A. Bourkba, M.F. Lautie, O. Poizat, Spectrochim. Acta 45A (1989) 187.